



## Advancing the morphometric analysis of early medieval Slavic pottery: A semi-automated 3D toolset for virtual sections

Martin Košťál <sup>\*</sup> , Vojtěch Nosek, Jiří Macháček

Department of Archaeology and Museology, Faculty of Arts, Masaryk University, Czech Republic



### ABSTRACT

This study introduces a semi-automated toolset for the generation of virtual cross-sections from 3D models of hand-made asymmetrical vessels. The toolset is presented through the analysis of early medieval Slavic pottery, with a particular focus on Prague-type ceramics. Developed using both visual and standard programming languages, the toolset extracts key morphometric attributes from 3D scanned pottery, facilitating a detailed analysis. To demonstrate its functionality, the toolset was used on 175 vessels from the Roztoky (CZ) and Přítluky (CZ) sites. For this initial demonstration of data extraction, commonly used morphometric attributes specific to early medieval Slavic pottery in Central Europe were employed, based on modified formulas from established typological systems. This open-source approach offers a fast and accurate solution for pottery analysis, advancing morphometric research in archaeology, especially that based on the automatic extraction of attributes from both 3D models and 2D sections.

### 1. Introduction

The morphology and morphometrics of ceramics are fundamental to the very beginnings of ceramic classification and represent one of the essential principles of the typological-chronological approach. Nevertheless, the morphometrics of pottery have applications that extend beyond the scope of typological-chronological analysis. For example, they can facilitate the classification of objects into functional categories, the interpretation of their original purpose and meaning within the context of the living culture, the identification of norms and binding behaviours (Bernbeck, 1997, 206 – with references) or the estimation of the degree of craft specialisation (Howard, 1981; Rice, 1981). In the absence of other distinguishing attributes, such as decoration or clearly differentiated technologies, morphology and morphometrics have become one of the primary methods in the research of (pre)historic ceramics, along side methods such as petrography, chemistry and many others, due to its cost efficiency.

Since the 1960s, numerical taxonomy methods have been utilized for the archaeological classification of ceramic shapes (Orton et al., 1993, pp. 152–165). These methods are applied not only to fragments but also to complete vessel shapes, which reflect the intended function of the vessel. Morphological parameters, such as volume, stability, and portability, directly influence the vessel's performance and its usage (cf. Shepard, 1971; Smith, 1985; Rice, 1987). The primary objective is to quantify the degree of similarity between vessels or their components in a numerically or graphically representative manner. Classical methods

of numerical taxonomy include, for example, cluster analyses (Hodson et al., 1971) or principal component analysis (Wilczek et al., 2014). More recently, the application of neural network and machine learning approaches (Gualandi et al., 2021; Demján et al., 2023) has allowed a larger number of ceramic shapes to be compared with greater efficiency. The situation seems much more optimistic than in the 1990s when archaeologists expressed disappointment that technological development seemed to hinder rather than help the relationship between analyst and pot (Orton et al., 1993, p. 163). Nevertheless, the most challenging aspect of measurement-based classification remains the accurate digital representation of a real pot.

It is evident, therefore, the initial step in the application of any numerical taxonomy method must be the acquisition of accurate data. Typically, published, scanned and digitised 2D drawings are utilized as the primary source of raw data (Wilczek et al., 2014; Loftus, 2022). However, this approach is not without limitations, particularly when examining handmade coarse wares, which are inherently non-symmetric and non-standardised in shape. An excellent example of such pottery is the so-called Prague type, which constitutes one of the most distinctive features of the Prague/Korchak culture. This ceramic, which is dated to the end of the Migration Period, has traditionally been associated with the Slavic-speaking population in Eastern and Central Europe (Rusanova, 1973, 1976; Fusek, 1994; Parczewski, 2004). The Prague-type pottery is typically characterised as a coarse and handmade ware and it's use spread across a vast area encompassing Ukraine, Belarus, Poland, Slovakia, the Czech Republic, Slovenia, Austria,

\* Corresponding author.

E-mail address: [462845@muni.cz](mailto:462845@muni.cz) (M. Košťál).

Germany, Hungary, Romania, and Greece during the 6th/7th centuries AD. The undecorated medium-sized pots (measuring 18–27 cm in height) with cylindrical open mouths and narrow, conspicuously thickened, bottoms were likely produced in households (Kuna and Profantová, 2005). The narrow and tall pots are shaped in a way that indicates optimal use in kiln cooking. The connection between kitchen culture and the similar shape of vessels is particularly evident in the Balkans (Pleterski, 2009).

Nevertheless, the association of Prague-type pottery with Slavic communities has been the subject of considerable criticism. It has been proposed that material culture, such as pottery and other artifacts, cannot be the primary indicator of Slavic identity (Curta, 2001). Furthermore, there is the additional challenge of defining Prague type pottery. As Florin Curta has noted, all of the existing classifications are based on ratios derived from basic measurements taken from 2D scale drawings of vessels or previously published vessel dimensions (Parczewski, 1993; Fusek, 1994, 30; Macháček, 1997, 359). Each of these classifications is based on the arbitrary selection of ratios to define classes, which makes the data collected in this way unsuitable for any multivariate analysis (Curta, 2021). In light of the aforementioned considerations, the aim of the present study is to develop a toolbox for the acquisition of accurate and, as far as possible, comprehensive digital data on handmade coarse pottery.

A critical component in the creation and retrieval of precise digital data from artifacts is their virtualization using modern documentation techniques. In recent years, the documentation of artifacts has made significant progress, particularly with the advent of 3D scanning technologies (cf. Kucukkaya, 2004; De Reu et al., 2013; Tsiafaki and Michailidou, 2015; Gajski et al., 2016; Novaković et al., 2017; Šindelář et al., 2019). These techniques not only accelerate the documentation process but also enhance its precision and, in many cases, allow for full automation of the process. Various approaches exist for analyzing 3D data of artifacts (Harush et al., 2019; Horn et al., 2019; Poigt et al., 2021; Gravel-Miguel et al., 2022; Mara and Bogacz, 2022; Di Angelo et al., 2024; Petrinelli Pannochia et al., 2024). One effective method for comparing and analyzing these data is through the creation of virtual cross-sections (cf. Karasik and Smilansky, 2008; Nosek and Kaňáková Hladíková, 2021; Thér and Wilczek, 2022). This approach is essentially an extension of the traditional procedure of segmenting artifacts into profiles, a technique that has been a cornerstone of shape analysis of artifacts since the field's inception.

Given the accessibility of 3D scanning tools—where even a basic smartphone can produce useable 3D scans with the usage of applications like RealityCapture, RealityScan, or Meshroom—it is surprising that, despite significant advancements in digital 3D documentation and morphometric analysis (cf. Bonhomme et al., 2014), the comparison of ceramic profiles still predominantly relies on traditional 2D section drawings. This approach, as seen in studies such as Wilczek et al. (2014), Wang and Marwick (2020), and Loftus (2022), essentially follows the same principles established decades ago (cf. Rusanova, 1973; Fusek, 1994; Macháček, 1997). However, one reason may be that the efficient and semi-automatic extraction of complex morphometric data is still challenging without advanced knowledge of programming languages (such as java, C# or R; see Badouel, 1990; Segura and Feito, 2001; Jiang et al., 2016). As a result, the practical applicability of these methods is often limited, even when the extracted data are intended for simple graphical description rather than in-depth analysis. Problems arise from the complexity of 3D data, high computational demands and the lack of available, user-friendly software solutions. Currently available open-source tools used in archaeology for processing and editing 3D data, such as CloudCompare, MeshLab, GigaMesh and Blender, do not offer intuitive semi-automatic or batch data extraction capabilities.

The goal of this paper is to introduce and describe concepts that will lead to a clearer workflow in the creation of virtual sections. It will outline the basic procedures for idealized serialization of 3D sections, introducing not only the extraction tools, but also highlighting the

possibilities and advantages of performing computations based on multiple virtual sections and extracting data directly from the 3D environment through a graphical user interface (GUI). The data obtained from this toolbox could be employed not only in the morphometric analysis of hundreds of vessels belonging to the Prague type, but also in the measurement-based classification of other pots of a similar nature.

## 2. Data and methods

### 2.1. Study data

The corpus used here comes from two sites in Czechia – a cremation burial ground in Přítluky (Poulík, 1951; Jelínková, 2012) and a megasite in Roztoky (Gojda, 1991; Kuna and Profantová, 2005; Kuna et al., 2013). The data were obtained from handmade undecorated vessels dated roughly between 500 AD to AD 800.

The pottery from Přítluky was infilled with plaster, in cases where fragments were missing, whereas the pottery from Roztoky was reconstructed from fragments without any infill. However, due to the methodology described below, these factors do not affect the analysis. Typological classification did not influence the selection in this case; though, it can be stated that the shape variability did not include any extremes, such as bowls, etc.

Although the vessels from each corpus are well-preserved and can be reconstructed from fragments, it was necessary to artificially limit the selection to complete or almost completed shapes, which were later 3D scanned and included only if at least 80 % of their circumference could be reconstructed. This need arises from the following methodological steps. A total of 55 scans of vessels were obtained from Roztoky, from which 40 samples were selected. From Přítluky, 160 vessels were scanned, and 135 were used in this study. In total, we analyzed 175 items (for shape variety of vessels see Fig. 1).

### 2.2. Data acquisition and pre-processing

For the purpose of morphometric analysis, the ceramic material was documented using two primary methods: image correlation (Structure from motion – SfM) and 3D scanning (structured light projection). The choice of documentation techniques was determined by the available equipment and the time constraints at each site. For the SfM (cf. De Reu et al., 2014; De Paolis et al., 2020), a Nikon D750 camera, featuring a 24.3-megapixel resolution and a 35.9 mm × 24 mm sensor, was employed alongside a Nikkor 60 mm f/2.8 G ED AF-S Micro lens mounted on a tripod. The ISO setting was fixed at 100, while the shutter speed and aperture were adjusted to match the specific optical and morphological characteristics of the artifacts. Typically, shutter speeds ranged from 1 to 1/6 s, with apertures varying between f/15 and f/20. The images obtained were subsequently processed using Agisoft Metashape software (cf. Nosek and Kaňáková Hladíková, 2021; Macháček et al., 2024). The photoshoot setup was used according to the procedure described by McCarthy (2014) with small changes forced by the inherent shape of the artifacts. For 3D scanning, an Artec Leo 3D scanner was used, along with its native software, Artec Studio 18, for raw data processing. The data acquired via structured light scanning achieved a resolution of less than 1 mm. All 3D data were normalized to this resolution and exported in standardized formats commonly used within the 3D modeling industry, such as .ply, .obj, and .fbx. This depends on the various needs of metadata storage. Once the data had been acquired, the 3D models were manually oriented in virtual space according to the orientation of the vessel's original stance (Fig. 2b), using the Z axis of 3D space for vertical direction.

The initial step of the analysis involved normalizing the 3D data using positional coordinate transformation, with the target set to the origin point (Fig. 2a–c). This transformation was performed without any axial rotation, as there were no rotation landmarks on the Z-axis. The



**Fig. 1.** Examples of the variety in shape and asymmetry of Prague-type pottery. From left: ROZTO\_3497\_209; ROZTO\_5152\_903; PRITL\_315; PRITL\_0\_CLXXXIV-362. 3D models visualised in Blender 4.1.

normalization process was applied automatically to all vessels and relied on the functional orientation of each vessel. Specifically, this process involved extracting the external bottom mass by selecting a set of bottom facets oriented along to the Z-axis ( $Z < 0$ ) and identifying the coordinate points where  $Z = Z_{\min} + x$ , with  $x$  representing the average distance between the inner and outer bottom surfaces. The arithmetic mean of the coordinates on each axis was then calculated to establish the functional center of the vessel, which was subsequently aligned with the zero coordinate in 3D space. Once the data had been centered, the next step involved extraction of first attributes from each 3D model - the inner and outer volume (cf. Zapassky et al., 2006).

### 2.3. 2D sections extraction

For the data extraction described below, the Blender software was used, especially its native visual programming language Geometry Nodes. The extraction of 2D section lines was based on principles of the Möller-Trumbore intersection algorithm (Möller and Trumbore 1997; this algorithm specifically calculates the intersection of any line (or ray) with any plane defined by a triangle in 3D space by solving a parametric equation to determine if and where the line intersects the triangle's plane and whether the intersection point lies within the triangle's bounds). This algorithm, implemented in Geometry Nodes (Higgsas, 2024), calculates the intersection points between the cutting plane and the 3D model's surface, which are subsequently used to generate the curve or section line. To retain as much of the original data as possible, both horizontal and vertical sections can be generated (cf. Thér and Wilczek, 2022; Slavíček et al., 2024) during the 3D-to-2D simplification process.

Horizontal sections can be created by linear displacement of the horizontal cutting plane along the Z axis. The number of cuts is defined by the required spacing between each horizontal cut, the maximum Z

size and the minimum Z size. The number of cuts of vertical slices is defined by angular distance on Z axis between each slice (see Fig. 2., d1-d3). For example, if 36 vertical sections were obtained, the angular distance between vertical sections is  $10^\circ$ . The origin of each vertical profile was determined by defining the axis of rotation (AoR) around which the cutting plane was rotated. This axis was established by first extracting the bottom surface of the vessel, based on its Z position and face normal orientation, and calculating the average of all x and y values to define the bottom center. To algorithmically automate this process for any given section, the sequence was repeated, allowing for the necessary shifts or rotations of the cutting plane based on a specified distance or angle parameters.

Since commonly used analyses of pottery primarily use only the outer line of a 2D section (Fusek, 1994; Kuna and Profantová, 2005; Wilczek et al., 2014; Wang and Marwick, 2020; Loftus, 2022) for the calculations, the division of the vessel attribute into inner and outer parts was included in the process of creating the 2D sections. This was achieved by analyzing the orientation of each facet in the 3D model using obtuse and acute angle searches. In principle, this involved calculating the angular deviation between the facet position, its center and the maximum height point (Fig. 2., f) in 3D space.

### 2.4. 2D section–principles of geomorphological attributes extraction

#### 2.4.1. Horizontal section processing

The extracted curves can be divided into horizontal and vertical sections, each of which requires a distinct approach for extracting metric information. Horizontal cross-sections describe attributes related to the concentricity and circumference of the vessel. In theory, each horizontal section consists of two curves: an inner and an outer circle. Dividing the section in this manner allows for the extraction of specific properties for each curve independently. Concentricity is defined as the distance

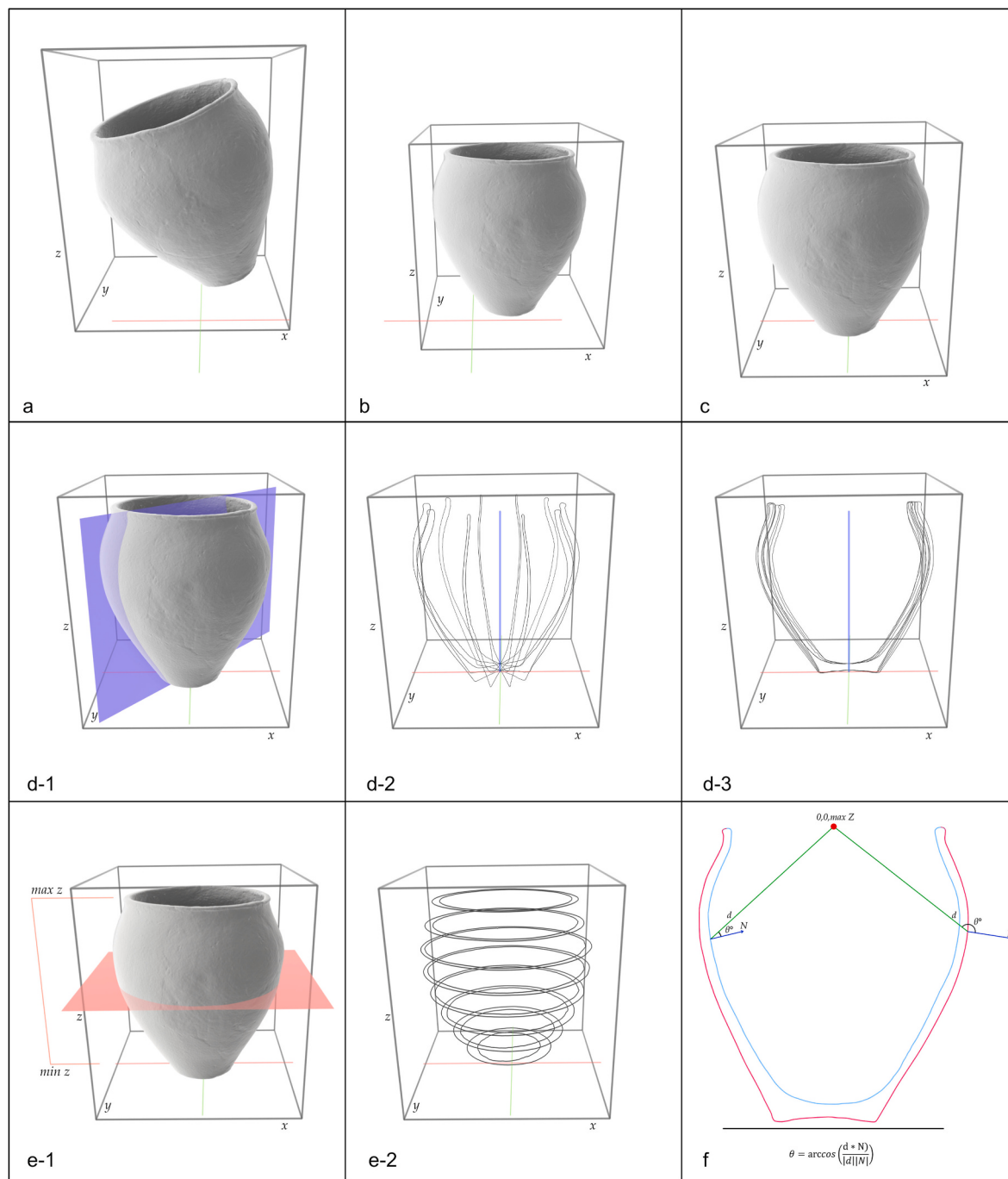


**Fig. 2.** Data orientation and sections extraction. **a)** Non-oriented 3D model; **b)** 3D model oriented according to the functional position; **c)** 3D model of the vessel transposed through the bottom center to the position 0,0, minZ - axis of rotation (AoR); **d-1)** Visualization of the vertical cutting plane; **d-2)** Visualization of the obtained vertical sections in the original position obtained by rotating the vertical cutting plane on the AoR (blue line) 10 times; **d-3)** Visualization of the vertical sections blended into 2D space using the backward rotation of the segment along the AoR; **e-1)** Visualization of the horizontal cutting plane; **e-2)** Visualization of the obtained horizontal sections with the distance between each cutting plane set to 5 cm; **f)** Schematic representation of the division of the vessel into inner and outer parts, where  $d$  = distance between the center of the surface/line and the point of maximum height(maxZ),  $N$  = normal of the surface/line;  $\theta$  = given degree. (For interpretation of the references to colour in this figure legend, the reader is referred to the Web version of this article.)

between the Axis of Rotation (AoR) and the median of the x and y values of the given horizontal slice, giving its name Concentricity of the outer/inner horizontal line (COHL/CIHL). This represents the deviation of the circle's center from the AoR. The circumference is then calculated based on the length of the line forming either the inner or outer circle.

#### 2.4.2. Vertical section processing

To compensate for shape variability across the vessel, all profiles

were rotated into a 2D z,y plane. Each section was rotated along the Z-axis by an angle corresponding to its initial orientation relative to  $0^\circ$  (e.g., section  $30^\circ$  was rotated by  $-30^\circ$  to align with  $0^\circ$ , see Fig. 2, d3). This provides sections divided into two halves - points whose coordinates at the y-axis are negative values and those with positive values. The next step was to translate all sections with points whose coordinates at axis y are lower than 0, to the half with positive y values. This was achieved by rotating those points along the AoR  $180^\circ$ . The basic principle of the

following steps involved dividing the sections into internal and external curves, as determined during the creation of the sections, and applying specific procedures to each inner or outer curve independently. Furthermore, each point of each section received an attribute of the percentage of its position along the y and z axis to provide a proportional filtering of the points. Those steps were calculated automatically in our study, based on given point attributes.

Vertical sections were subjected to a metrical taxonomy focused on attributes derived from commonly used systems for the study of early medieval Slavic pottery (cf. Rusanova, 1976; Fusek, 1994; Kuna and Profantová, 2005; see Fig. 3) and for pottery in general (Thér and Wilczek, 2022). These attributes are basically distance-based parameters (e.g. maximum diameter of vessel body). To detect them, it is necessary to find descriptive points, which are defined by the dimensional properties of the curve and parameters determined by the curve's characteristics, such as its inflection points. The defined points are named as follows:

P1 – lowest bottom point, P2 – largest bulge of the lower body, P3 – largest bulge of the body, P4 – largest bulge of the shoulders, P5 – narrowest part of the neck/rim. Wall thickness is considered as a separate attribute.

For the automated identification of P1, it was necessary to identify the inflection points of the refractive curve. This was achieved by mathematically identifying the points where the curve transitions from positive to negative and vice versa. The underlying method relies on the second derivative of the equation  $y = f(x)$ , with the optimal result being zero (cf. Nicholas, 2004). Given the nature of the data and the need for intuitive calculations, the basic equation was modified and algorithmically optimized to define the curve's nature based on the angular deviation of each line (Fig. 3). The P1 point, located at the lowest inflection point, was defined as being at least 5 % away along the y-axis. The distance from the center along the y-axis is crucial due to the uneven nature of the pottery.

Further classification points (P2-P5) of the vessel required defining several distance-based points. Standard 2D space calculations were applied, based on the 2D position statistics of known elements. This approach enabled the identification of the point P3, defined as the point farthest along the y-axis from the center axis of the body region. The

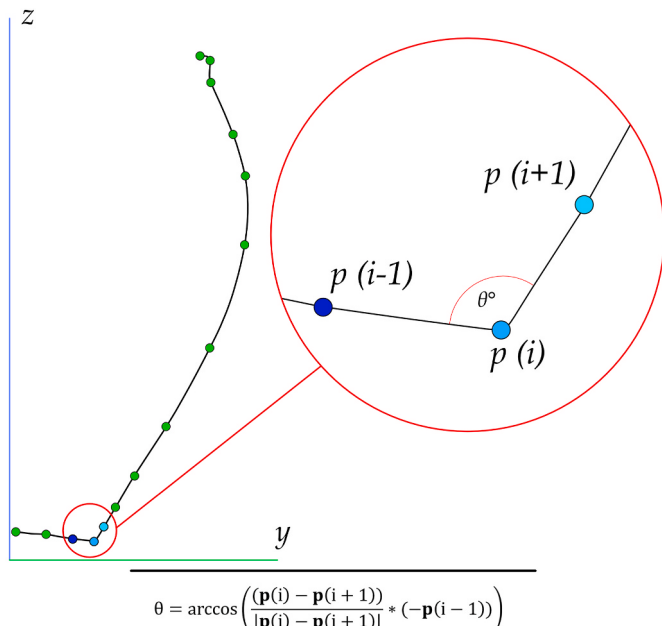


**Fig. 3.** Schematic representation of the iteration of the algorithm for determining the angular deviation (inflection point) on a 2D line, where  $p$  = position,  $i$  = index of the point,  $\theta$  = given degree.

point P5 was defined by identifying the closest point to AoR at the y-axis and its z% is equal to 80 %, or more.

The next metric attribute analyzed was the point P4. This attribute was automatically extracted by selecting the part of the section bounded by points P5 and P3. By calculating the arccosine using the Z- and Y-axis segments between points P5 and P3, an angle was obtained that allowed the rotation of the transect so that the point of greatest vorticity was farthest from the AoR. Back-rotation placed the point at its original position. The same procedure was used to identify the largest bulge in the vessel body (P2), using points P1 and P3 to obtain the angle of rotation. Given the strong positional variability of individual points, caused by the heterogeneity of the individual sections, the arithmetic median for each point P1-P5 was calculated for each vessel (Fig. 4-c).

The final metric attributes extracted from the vertical profile included wall thickness (WT), the mean height of the vessel, and the concentricity of the outer and inner lines (COL/CIL). Wall thickness was calculated by selecting the inner curve of the section, thickening it to include one point every 1 mm, and projecting lines from these points onto the outer curve at a +90° angle to the tangent. The mean height of the vessel was determined by averaging the maximum height across all sections. The COL/CIL attribute was defined as the distance between two points at each 1 mm interval along the z-axis: one with the lowest y-axis coordinate and the other with the highest y-axis coordinate. This attribute provides an alternative to the COHL/CILH attribute.

All these attributes are extracted into a .csv format using a Python console, implemented in Blender software (the extracted dataset is part of the supplementary data). The Python script works by accessing the attribute table from GN (Geometry Nodes) and then converting it into a .csv format using the Pandas and Numpy libraries.

## 2.5. Analysis of the accessed attributes

### 2.5.1. Numerical analysis based on classical typology

For the purposes of further calculations, 36 cross-sections were created for each vessel, defining both vertical and horizontal attributes. In the basic numerical analysis, formulas were used to obtain length-to-width indices for early medieval pottery, based on the principles of Zoll-Adamikova (1977) and modified by G. Fusek (1994, 32–34) – formulas named A, H, and M (see Fig. 3-a). In principle, these formulas were designed to use only the positive half of the 2D y and z space (see Fig. 3-c). Since the distance attributes were calculated based on detected points P1-P5 and the maximum Z size of the 3D model, it was necessary to modify the notation of the individual formulas for the purposes of this study.

For the basic classification of the vessels into the existing categories of Korchak, Tushemly-Kolochin, and Penkovka (Rusanova, 1976), formula A was used, which after modification appears as follows:

$$A = A1 : A2; A1 = [P3z : MaxZ]; A2 = [2(P5y) : 2(P3y)]$$

The H formula for determining the length-to-width indices of pot-shaped vessels and the M formula for determining the length-to-width indices of bowl-shaped vessels are as follows:

$$H = H1 : H2; H1 = [2(P1y) : 2(P5y)]; H2 = [2(P3y) : MaxZ]$$

$$M = M1 : M2; M1 = [2(P1y) : (P5y)]; M2 = [MaxZ : 2(P3y)]$$

These formulas enable the comparison of pot-shaped vessels within a modified diagram, where it holds that – if  $H2 > 1$ , the M formula is used for the length-to-width indices. The values obtained in this way allow the plotting of the calculated indices into a graph, where  $H1/M1$  represents the vertical axis and  $H2/M2$  represents the horizontal axis.

### 2.5.2. Computation of production process similarity

To test the similarity of individual vessels in terms of production techniques and to compare these results with existing classifications (cf. Fusek, 1994, 32–34), several qualitative variables, termed production

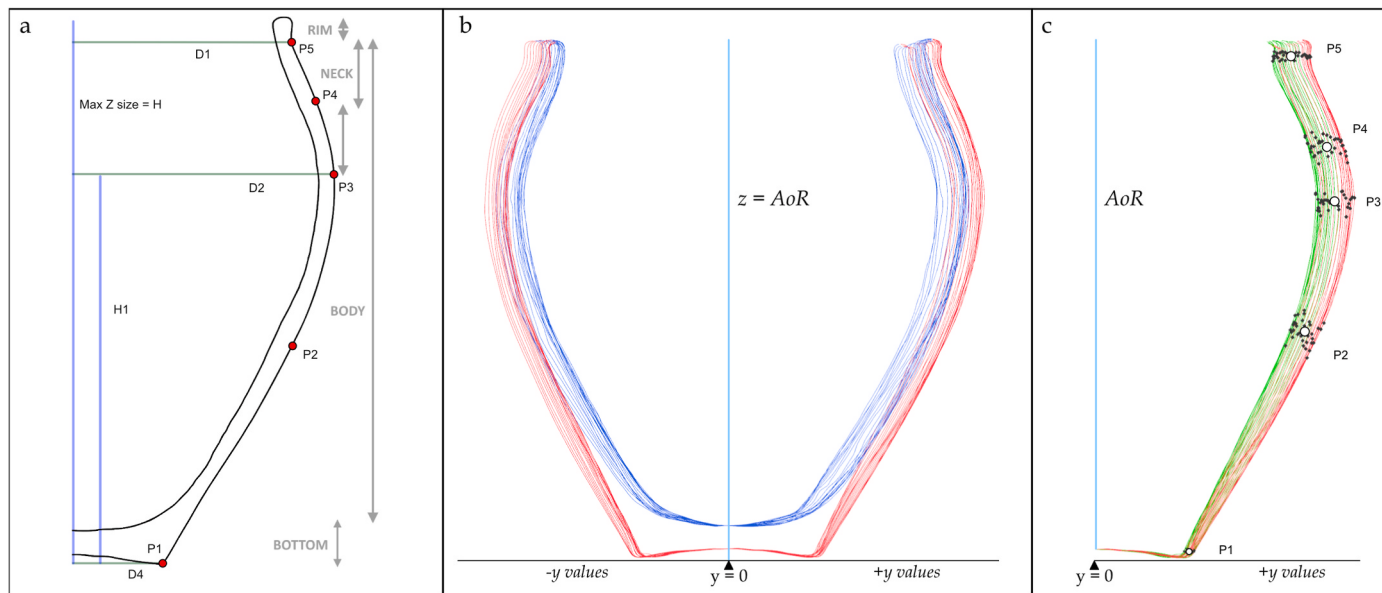


**Fig. 4.** Accessed attributes and basic principles of curve transferring. a) Main curve points and vessel measurements; b) 36 sections converted to 2D space with inside/outside line separation; c) Automatically defined points P1–P5 and their approximation to the arithmetic median (red points). Green lines represent outer lines converted from -y coordinates to +y coordinates. (For interpretation of the references to colour in this figure legend, the reader is referred to the Web version of this article.)

markers, were defined based on data extracted from 3D models. These variables are relevant to the production process. The first marker is the concentricity of the outer line (COL), and the second is wall thickness (WT). Both markers were divided into four categories based on their percentage distance along the z-axis (pz%) relative to the categorical descriptors P1–P5. The categories for wall thickness were defined as follows: WT1, base thickness ( $pz\% \geq P1z\% + 10\%$ ), WT2, lower body wall thickness ( $P1z\% > pz\% < P3z\%$ ), WT3, vessel bulge thickness ( $P5z\% > pz\% < P4z\%$ ), and WT4, rim thickness ( $P5z\% + 5z\% > pz\%$ ). The same proportional calculations and naming procedure was used for COL attribute. These eight variables were considered alongside the H1/M1 and H2/M2 indices as well as the inner and outer vessel volume.

The degree of resemblance between vessels was determined by computing the similarity distance for the 12 descriptors mentioned above. Similar to previous work (Wilczek et al., 2014), Gower's distance (Gower, 1971) was used to define the similarity coefficient  $S_{ij}$  between two individuals. The computation was based on the following formula:

$$S_{ij} = \frac{\sum_{k=1}^p \omega_{ijk} s_{ijk}}{\sum_{k=1}^p \omega_{ijk}}$$

Where the distance  $S$  between two individuals  $i$  and  $j$  is calculated for  $p$  variables. Therefore,  $g_{ijk} = 1_{g_{\{ijk\}}} = 1_{g_{ijk}} = 1$ , for values defining the level of the formation process the weight has been multiplied up to three times. In particular, the wall thickness (WT 1–4) of the vessel in the area of the bottom and the lower part of the vessel body had more weight in the analysis than the wall thickness in the area of the rim and shoulders. This decision employed the premise, based on the forming process of ceramic vessels, that the thickness of the rim and shoulder is always equal to or less than the thickness of the base. Another descriptor used was the concentricity (COL 1–4) of the vessel. It can be assumed that the larger the vessel is, the more likely the top of the vessel will be non-concentric. It is for this reason that a higher weight was assigned to the upper parts of the vessel.

Kronecker delta  $\delta_{ijk} = 0_{w_{\{ijk\}}} = 0_{w_{ijk}} = 0$  was employed when information is missing. A metric multidimensional scaling, also known as Principal Coordinates Analysis (PCoA), was computed to visualize the level of similarity. The transformed dissimilarity matrix  $\sqrt{D} = 1 - S$  was preferred for the computation, as it is less likely to generate negative

eigenvalues (Legendre and Legendre, 1998). Implementation of this statistical method was processed in R software (the code is part of the supplementary data at Zenodo repository - Košfál et al., 2025).

In order to monitor the differences between the traditional numerical analysis described above and the difference based on formation processes, the calculation of the dissimilarity of the attribute H index was used. For that purpose the weight of attributes H1 and H2 was the same.

### 3. Results and discussion

#### 3.1. Algorithm implementation to mesh section toolbox

The long-term sustainability of software should be a key consideration. Although algorithms for cross-section generation have existed for some time, their application remains limited, likely due to hardware constraints and limitations in current software. Many GUI-based tools offer only basic functionality, limiting workflow optimization. In contrast, advanced libraries without GUIs require programming skills, reducing accessibility. Furthermore, many GUI extensions are closed-source or poorly documented, complicating automation and the consistent segmentation of multiple 2D slices from 3D models.

Several software tools, such as Blender, CloudCompare, and GigaMesh, support cross-section generation from 3D models by intersecting section planes with models. These tools vary in the intersection techniques employed: ray tracing determines intersection points via surface ray tracing (cf. Möller and Trumbore 1997; Segura and Feito, 2001; Baldwin and Weber, 2016), while Boolean operations perform calculations for intersections, unions, or geometric differences (cf. Nievergelt and Preparata, 1982; Jiang et al., 2016; Geng et al., 2024). Algorithm selection is complex due to differences in computational speed and consistency.

Blender was selected as the primary tool for this study, as it offers a GUI with extensive customization due to its open-source nature. An open-source GN toolset was developed to optimize archaeological 3D data by implementing a surface and point intersection algorithm (Möller and Trumbore 1997; cf. Higgsas, 2024), enabling fast and accurate section cuts. The toolset consists of four tools: *the pottery section generator*, *general section generator*, *section analysis*, and *attribute exporter*. The pottery generator handles 3D pottery scans, assuming a central

rotational axis and functional vessel orientation, while the general section generator enables interactive artifact sectioning without requiring artifact orientation.

Testing revealed that Boolean algorithms were slower than raycasting algorithms for section cuts. Blender's MeshBoolean tool, tested in GN (see [Blender, 2024](#); cf. [Slavíček et al., 2024](#)), required several minutes per model under the same conditions where the Möller-Trumbore algorithm ([Möller and Trumbore 1997](#)) processed in seconds, with similar accuracy. Section analysis allows attribute extraction, with a Python script for .csv export. Although algorithms using five description points (P1–P5) perform consistently, high variability occasionally requires manual adjustments, especially in high-density scans.

Tested on 175 vessels, this toolset conceptually resembles GIS-based extensions, streamlining workflow to a few variables and enabling rapid data extraction, with each model processed in seconds. The algorithm is published under a CC 3 license on Zenodo ([Košťál et al., 2025](#)).

Although this implementation provides reliable data results for pottery, it is evident that the presented workflow for curve extraction can also be applied to other artifacts. Specifically, the general application of horizontal sectioning can be utilized on virtually any artifact. With minor modifications to the logical operations in the code—such as adding a separate input for the target geometry and a plane whose normal represents orientation in space and whose coordinates define the relative point of the axis of rotation (AoR) - it becomes possible to extract curves from any artifact at any point in 3D space. The analysis and attribute extraction from these curves is a separate topic, as the presented workflow was specifically designed for complete vessel shapes.

### 3.2. Numerical analysis

The classical numerical analysis of length-width indices enabled the creation of comparative diagrams between Early Slavic pottery from the territories of the Czech Republic and the Slovak Republic ([Fusek, 1994](#)). For the comparison, diagrams were used where the vertical axis represents the results of H1/M1/A1, and the horizontal axis represents H2/M2/A2. The boundaries of the individual ceramic classes/types are based on the values defined by [G. Fusek \(1994, 22\)](#).

When classifying the vessels from the Přítluky and Roztoky sites into basic classes (Fig. 5), it is evident that the majority of the data falls into group I - Korchak (roughly 70 %), according to Rusanova ([Rusanova, 1973, 1976](#)), who conducted the archaeological analysis of the Early Mediaeval pottery from the region between the Dnieper, Pripyat and

Dnester rivers on the territory of present-day Ukraine and Belarus. Group I is defined as the so-called Prague/Korchak type, which is, in view of Rusanova, synonymous with Early Slavic pottery from the territory of northern and central Ukraine. The specific morphometric features that define this type include the ratio between the diameter of the neck of the vessel and the maximum diameter of the body, as well as the ratio between the full height of the vessel and the height of the maximum diameter of the body. The Korchak type is distinguished from other types of Early Slavic pottery, such as the Penkovka and Kolochin types, by these parameters ([Fusek, 1994, 20–23](#)). This distribution across the individual categories can be favorably compared with the results of manual measurements, both for the vessels from the Přítluky site ([Kuna and Profantová, 2005, Fig. 54c](#)) and for the vessels from the Roztoky site ([Kuna and Profantová, 2005, Fig. 54c](#)). A similar data distribution (i.e., into category I and III) is also consistent for early medieval pottery from the Slovak region ([Fusek, 1994, Fig. 4](#)). When the data are compared using the H1/M1 index into classes A-D and the H2/M index into classes I-II (see Fig. 6), it can be observed that vessels from the Czech Republic exhibit less variability in H1 values. However, similar to the vessels from Slovakia, they are predominantly clustered in classes B I, B II, and C I, C II. The pottery from Roztoky site, in particular, corresponds predominantly to category B II, although the majority of vessels from Přítluky also fall within the same category. Based on this comparison, it is evident that the evaluated data are characterized by globular pots with similar outer base widths and neck widths.

The defined threshold values in the diagram, based on formula A according to [G. Fusek \(1994, 33\)](#), divide the vertical part of the diagram into values 1–3, and the horizontal part into a and b (Fig. 7). The left side of formula A (A1) defines the position of the greatest bulge relative to the total height of the vessel. The larger the number, the higher the greatest bulge is positioned on the pot. The pot-shaped and bowl-shaped vessels examined in this study typically have the largest bulges located in the second and third sixths of the vessel's height. The right side of formula A (A2) indicates the ratio of the neck diameter to the diameter of the greatest bulge. Wider necks have a higher A2 value, while narrower necks have a lower value.

In this comparison, even more significant differences can be observed between vessels from the Roztoky site, which mostly correspond to group 1b, and the Přítluky site, where the vessels predominantly fall into group 2b. Based on the presented formulas, a high level of homogeneity can be observed in the vessels from the Roztoky site, whereas the vessels from Přítluky exhibit greater heterogeneity, although they tend to cluster within a single type. These findings are

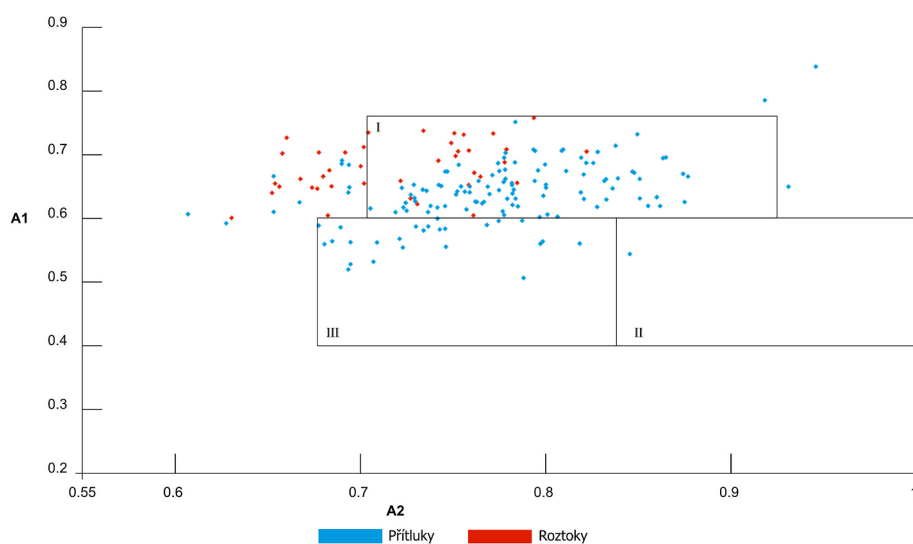


**Fig. 5.** Proportion diagram, based on the calculations of formula A, with the overlap of the original definitions by I.P. Rusanova. (Axis A2 scaled 3x in accordance with Fig. 4, [Fusek, 1994](#)). I - Korchak, II - Tushemlya-Kolochin, III - Penkovka.

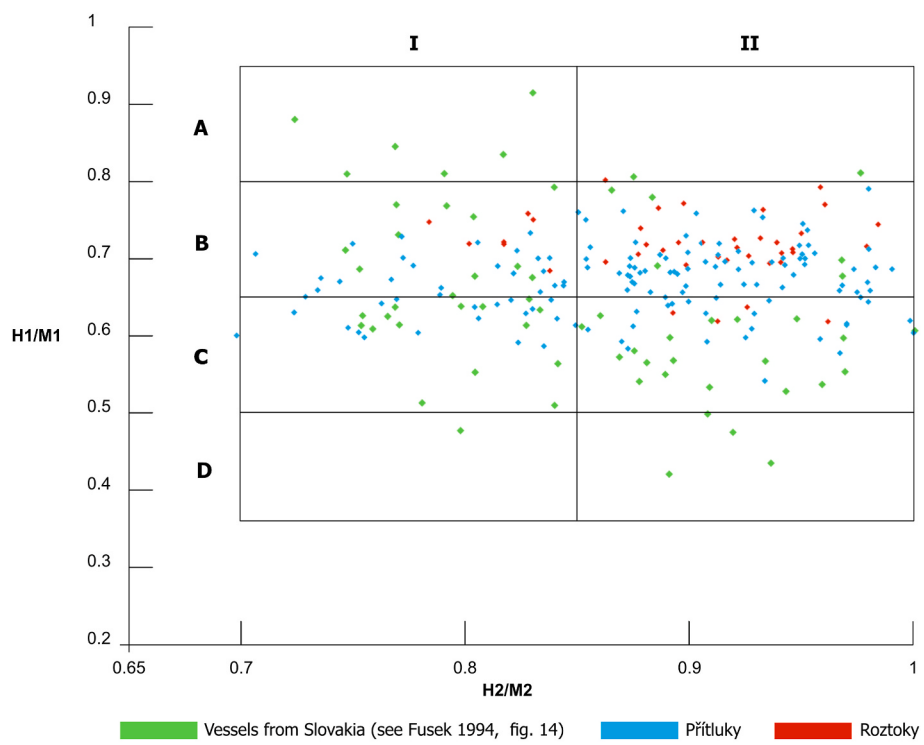


**Fig. 6.** Proportion diagram, based on the calculations of the H/M formula (cf. [Fusek, 1994](#)).

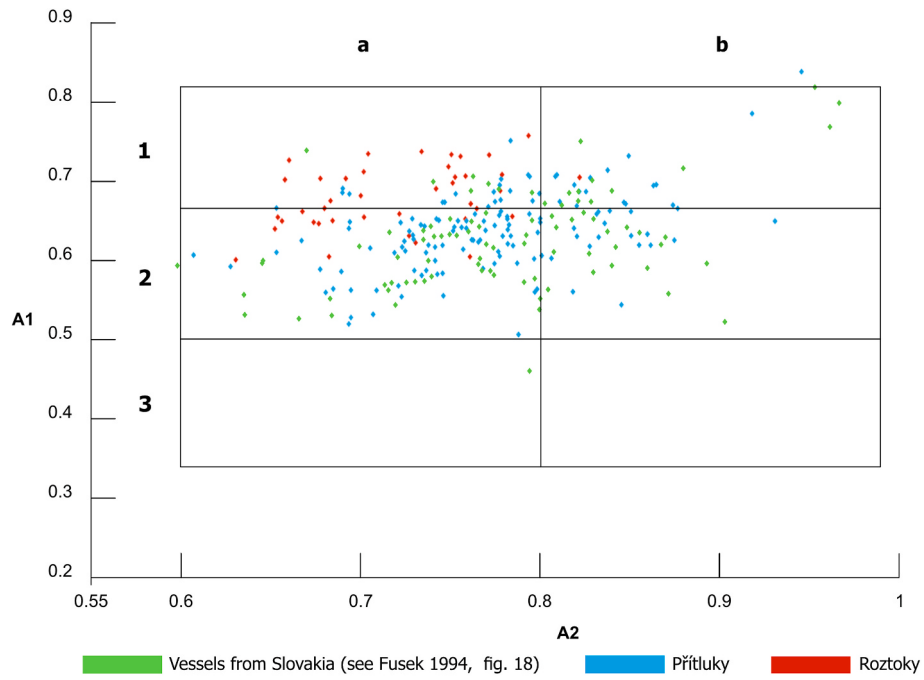


**Fig. 7.** Proportion diagram based on the calculations of formula A (cf. [Fusek, 1994](#)).

broadly in line with previously published studies ([Kuna and Profantová, 2005](#), 154–156) and confirm that autonomously generated calculations based on data derived from 3D models have sufficient potential to quickly extract accurate metric data. It is important to keep in mind that any comparison between newer and older technologies can only demonstrate overall similarity of the material. Since the presented workflow for attribute acquisition and its analysis is based on median points, slight differences may occur. To address this, it would be necessary to create a calibration matrix based on the same robust

dataset, utilizing both old and new approaches.

### 3.3. Similarity computation of production process based on Gower's distance

The obtained Gower's constant values, plotted in 3D space (see [Fig. 8](#)), not only offer a fresh perspective on shape comparison as defined by [G. Fusek \(1994\)](#), but also reveal that the automatically defined attributes P1–P5, along with the variables H1/H2 derived from them,

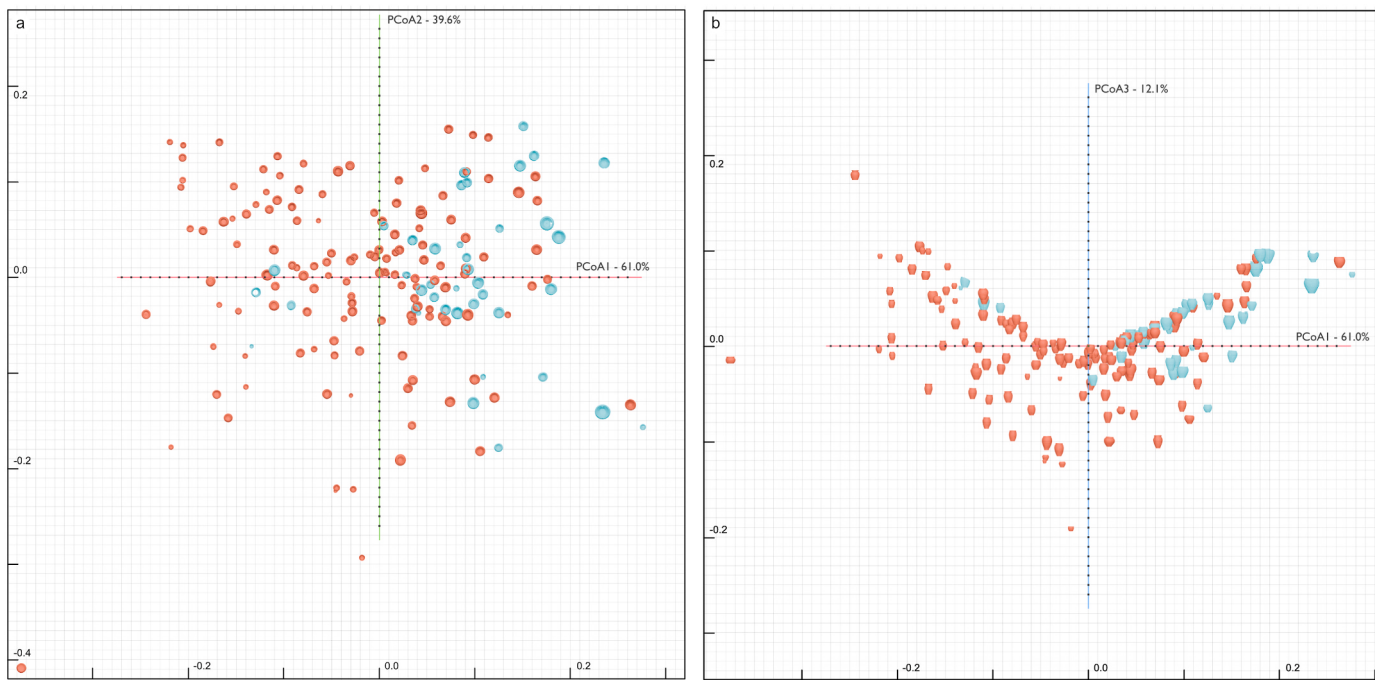


**Fig. 8.** Shape classification based on the H-index, with differences calculated using PCoA and Gower's distance: a) Axis 1 and 2, b) Axis 1 and 3. 3D graph available at: <https://sketchfab.com/3d-models/supplementary-data-1-shape-similarity-80ffd3b7197423ba42894d2587659fb>.

enable surprisingly intricate shape comparisons. Although the Gower distance matrix is not Euclidean, the resulting 3D graph produced through Principal Coordinates Analysis (PCoA) effectively captures and represents the relationships between individual vessels. The spatial arrangement in the 3D projection aligns well with the expected typological and morphological groupings, demonstrating that the analysis provides a meaningful visualization of the data structure. Despite the presence of non-Euclidean characteristics, the key patterns and

similarities among the vessels remain clearly interpretable within the reduced dimensional space. This is notable despite these values representing only medians, without accounting for intrinsic vessel variability. Although the sample presents as relatively homogeneous, its internal heterogeneity is considerable, evidenced by the presence of several smaller, localized vessels within the graph. The extent of dissimilarity is particularly evident by the distance from other vessels in the sample, with the bowl-shaped vessel PRITL\_460\_P-CCL standing out, entirely

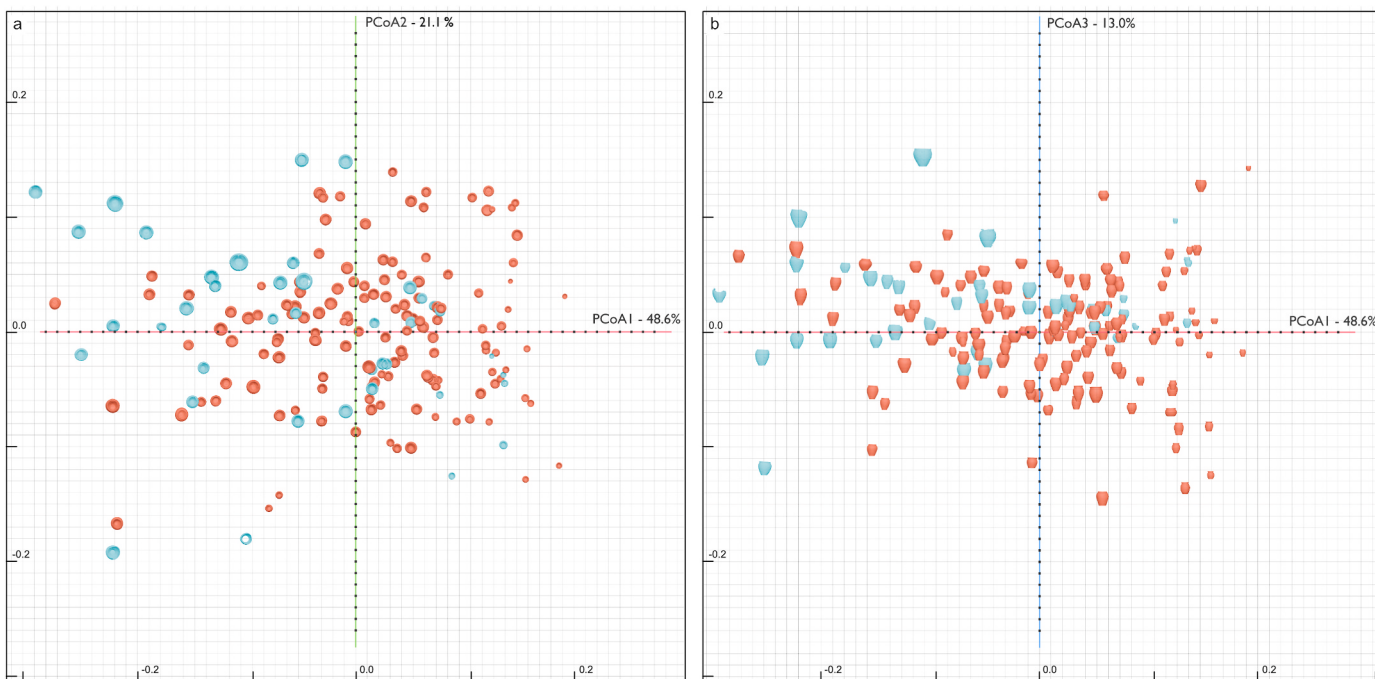


**Fig. 9.** Analysis of production markers based on the H-index, wall thickness, vessel concentricity, and vessel volume. Differences calculated using PCoA and Gower's distance: a) Axis 1 and 2, b) Axis 1 and 3. 3D graph available at: <https://sketchfab.com/3d-models/supplementary-data-2-technological-similarity-6f3258a82d9c4360b5159fd9675b31b4>.

isolated from other clusters. Despite some overlap in shape variability between the Roztoky and Přítluky assemblages, Přítluky pottery exhibits greater shape diversity.

A different perspective emerges when comparing the assemblages based on production-related ceramic characteristics, such as concentricity and wall thickness (Fig. 9). This comparison reveals greater homogeneity across the assemblage. While typological differences, measured by the H-index, are apparent, greater emphasis is placed on base thickness and rim concentricity. The calculation of differences based on production markers revealed that all types of vessels (i.e., barrel-shaped, cauldron-shaped, and bowl-shaped) are quite similar, to a certain extent, and span a broad spectrum without clear clustering. However, even within these categories, it is possible to observe differences between settlement pottery from the Roztoky site and funerary pottery from the Přítluky site. The most significant difference is seen in the high COL values, which are characteristic not only of large vessels but also of smaller ones.

Although traditional typology might be considered insufficient, given that it takes into account only certain aspects of shape variability and does not allow for detailed statistical evaluation (Bonhomme et al., 2014), previous tests have demonstrated good statistical concordance between morphology and numerical analysis based on typological classifiers (Wilczek et al., 2014). Moreover, it should be noted that standard procedures for comparing ceramic morphology (Wilczek et al., 2014; Wang and Marwick, 2020; Loftus, 2022) involve pottery produced on fast-turning wheels or at least wheel-thrown vessels. This approach allows for comparison based on just one profile. However, the significant internal shape heterogeneity of hand-modeled vessels precludes the use of this approach, as the variability among individual sections within a single vessel is substantial.

A deeper and more detailed understanding of the morphology of Early Slavic medieval pottery and its analysis remains a separate issue, lying beyond the scope of this study, which primarily focuses on data generation. Nevertheless, the results presented here highlight the potential of simplifying 3D models into 2D slices. The combination of well-established classification systems for 2D slices with accurate 3D modeling techniques has proven effective. The extracted attributes could be further expanded to include advanced methods such as the incorporation of inner curves of the vessels into analyses, the automated classification of several pottery components (such as detailed description of upper parts based on angles), or even Fourier curve transformation analysis (cf. Wilczek et al., 2014; Thér and Wilczek, 2022). It is important to keep in mind that morphology is only one of the key elements of pottery research and should be combined with other methods, such as petrology, microscopy, lipid analysis, and more.

For the automated identification of points P1–P5, the presented approach requires data standardization. Since the described identification methods also rely on proportional identification, it is essential to have vessel geometry that includes the complete overall height of the vessel (from rim to bottom). In cases where fragmentation or missing parts of the vessel body occur, the accuracy of point identification may be affected. However, as each point is defined as the arithmetic median for the given vertical section, it remains robust against outliers. Another limitation of proportional identification is the need for handleless pottery, as the presence of handles could distort the y% attribute. To address this, additional logical operators and inputs would need to be implemented to adjust or exclude conflicting geometry data. Nevertheless, despite these limitations, the general application is adaptable to any type of pottery. For a complete understanding of the tool and its functionality, please refer to the [GitHub page](#) (see Data availability statement) and its accompanying manual.

#### 4. Conclusions

This study introduces a semi-automated toolset designed for generating virtual cross-sections of 3D models, with an initial application to

early medieval Slavic pottery, particularly Prague-type ceramics. Developed using Blender's Geometry Nodes and Python, the toolset enables the extraction of key morphometric attributes, such as wall thickness, concentricity, and overall shape profile, directly from 3D scans. This approach allows for a detailed and nuanced analysis that overcomes the limitations of traditional 2D methods, which often struggle with non-standardized, hand-modeled artifacts.

Applied to 175 vessels from the sites of Roztoky and Přítluky, the toolset facilitated comparisons using both classical typological formulas and modern similarity measures, including Gower's distance and Principal Coordinates Analysis (PCoA). These methods underscored the efficiency and accuracy of the toolset, showing its ability to provide consistent, reproducible classifications and deeper insight into shape variability and production techniques across different ceramic types by shape extraction. The results of these analyses revealed significant differences in pottery between the two sites, highlighting distinct trends in burial and settlement contexts. Importantly, the open-source nature of this toolset allows for a high degree of customization, making it accessible to researchers with minimal programming experience. Presented analysis of non-symmetrical, handmade pottery demonstrated the potential of this toolset to address longstanding challenges in ceramic morphometrics. However, it is also possible to extract only the shapes and all measurements without calculating medians, allowing for the application of alternative analytical approaches.

The presented toolset represents a substantial advancement in the digital analysis of morphometric data, offering archaeologists a flexible and accurate approach to studying artifacts. While tested primarily on early medieval Slavic pottery, its applications extend far beyond ceramics. This toolset can be adapted to analyze a wide variety of archaeological artifacts, regardless of material, shape, or construction technique. By enabling the extraction of morphometric attributes from any 3D model, this toolset provides a robust framework for the quantitative analysis of artifacts across different cultural and historical contexts.

The benefits of this tool are particularly evident in its capacity to handle the complex shapes of hand-modeled objects, which often display considerable internal variability. Unlike traditional analysis methods that rely on a single profile view, this toolset generates multiple cross-sections, offering a comprehensive representation of the artifact's morphology. Additionally, the toolset's reliance on Blender's open-source platform allows for both broad accessibility and flexibility, inviting future enhancements and adaptations for various research needs.

By advancing workflow efficiency and improving data consistency, this toolset bridges the gap between digital 3D modeling and traditional morphometric analysis. It holds potential not only for enhancing archaeological typologies but also for supporting new methodologies in material culture studies. Future developments could focus on refining the tool for even more specialized applications, such as artifacts with high fragmentation or complex surface geometries. However, it is important to keep in mind that morphological data is only one of the available methods for pottery research and should be used alongside other approaches, such as petrography, archaeological context, lipid analysis, and more. In summary, this toolset offers a practical, adaptable, and precise solution for researchers aiming to conduct detailed morphometric analyses, making it a valuable addition to the archaeological and broader heritage research toolkit.

#### CRediT authorship contribution statement

**Martin Košfál:** Writing – review & editing, Writing – original draft, Software, Formal analysis, Visualization, Methodology. **Vojtěch Nosek:** Writing – original draft, Methodology, Supervision, Data curation. **Jiří Macháček:** Writing – review & editing, Methodology, Writing – original draft, Project administration, Funding acquisition.

## Data availability statement

All extracted data from the 3D models of the Roztoky and Přítluky sites, including the developed toolbox and example files, are available via Zenodo (Košťál et al., 2025):

[https://zenodo.org/records/15411117?token=eyJhbGciOiJIUzUxMiJ9.eyJpZCI6IjY5Njg4MzYxLTNmMGEtNDE4Ny04ZGYOLTg0YTNhMzBjODY0YSImRhdGEiOnt9LCJyYW5kb20iOlxNxQzZTQ2ZmIwNGY0ZWExMDU0ZjIwZTQ1MGY0ZmEwOCJ9.sZ7q0t1dkYANvXns2PHwFdplGquvN2TA11QQ9MnfTkfg4Al7swTgwtCymPWWLhi9BXJGW9q9w-b2wZ4j\\_RP-Q](https://zenodo.org/records/15411117?token=eyJhbGciOiJIUzUxMiJ9.eyJpZCI6IjY5Njg4MzYxLTNmMGEtNDE4Ny04ZGYOLTg0YTNhMzBjODY0YSImRhdGEiOnt9LCJyYW5kb20iOlxNxQzZTQ2ZmIwNGY0ZWExMDU0ZjIwZTQ1MGY0ZmEwOCJ9.sZ7q0t1dkYANvXns2PHwFdplGquvN2TA11QQ9MnfTkfg4Al7swTgwtCymPWWLhi9BXJGW9q9w-b2wZ4j_RP-Q)

Due to size and legal limitations, the original 3D models are available upon reasonable request from the corresponding author.

Ongoing development of the toolset is available at: <https://github.com/ArchaeoComp/MeshSectionToolset>.

## Declaration of generative AI and AI-assisted technologies in the writing process

During the preparation of this work the authors used ChatGPT in order to optimize the language and python/R code of the script. After using this tool/service, the author(s) reviewed and edited the content as needed and take(s) full responsibility for the content of the publication.

## Declaration of competing interest

The authors declare that they have no known competing financial interests or personal relationships that could have appeared to influence the work reported in this paper.

## Acknowledgment

This paper was financed by the research grant GAČR EXPRO GX21-17092X (The Formation of Multi-ethnic Complex Societies in Early Medieval Moravia. Collective Action Theory and Interdisciplinary Approach)

We would like to sincerely thank the Institute of Archaeology of the Czech Academy of Sciences in Brno, specifically Lumír Poláček and Marián Mazuch, as well as the Institute of Archaeology of the Czech Academy of Sciences in Prague, namely Martin Kuna, for their willingness and for providing access to materials for the purposes of scanning, virtualization, and documentation. We also extend our gratitude to Ian Randall for his valuable insights.

## References

- Badouel, D., 1990. An efficient ray-polygon intersection. In: *Graphics Gems*. Academic Press Professional, Inc, USA, pp. 390–393.
- Baldwin, D., Weber, M., 2016. Fast ray-triangle intersections by coordinate transformation. *JCGT* 5 (3), 39–49. <http://jcgtr.org/published/0005/03/04/>.
- Bernbeck, R., 1997. Francke Verlag. Tübingen, Germany.
- Blender, 2024. [https://docs.blender.org/manual/en/4.1/modeling/geometry\\_nodes/mesh/operations/mesh\\_boolean.html](https://docs.blender.org/manual/en/4.1/modeling/geometry_nodes/mesh/operations/mesh_boolean.html).
- Bonhomme, V., Picq, S., Gaucherel, C., Claude, J., 2014. Momocs: outline analysis using R. *J. Stat. Software* 56 (13), 1–24. <https://doi.org/10.18637/jss.v056.i13>.
- Curta, F., 2001. The Making of the Slavs: History and Archaeology of the Lower Danube Region, C, vol. 52. Cambridge University Press, Cambridge, pp. 500–700. <https://doi.org/10.1017/CBO9780511496295>.
- Curta, F., 2021. Slavs in the Making: History, Linguistics, and Archaeology in Eastern Europe (Ca. 500 – Ca. 700). Routledge, London – New York.
- Demján, P., Pavík, P., Roosevelt, C., 2023. Laser-aided profile measurement and cluster analysis of ceramic shapes. *J. Field Archaeol.* 48 (1), 1–18. <https://doi.org/10.1080/0934690.2022.2128549>.
- De Paolis, L., De Luca, V., Gatto, C., D'Errico, G., Paladini, G., 2020. Photogrammetric 3D reconstruction of small objects for a real-time fruition. In: Proceedings of the 22nd International Conference on Virtual Systems and Multimedia (VSMM), pp. 375–394. [https://doi.org/10.1007/978-3-030-58465-8\\_28](https://doi.org/10.1007/978-3-030-58465-8_28).
- De Reu, J., Plets, G., Verhoeven, G., De Smedt, P., Bats, M., Cherretté, B., De Meyer, W., Deconynck, J., Herremans, D., Laloo, P., Van Meirvenne, M., De Clercq, W., 2013. Towards a three-dimensional cost-effective registration of the archaeological heritage. *J. Archaeol. Sci.* 40 (2), 1108–1121.
- De Reu, J., De Smedt, P., Herremans, D., Van Meirvenne, M., Laloo, P., De Clercq, W., 2014. On introducing an image-based 3D reconstruction method in archaeological excavation practice. *J. Archaeol. Sci.* 41, 251–262. <https://doi.org/10.1016/j.jas.2013.08.020>.
- Di Angelo, L., Schmitt, A., Rummel, M., Di Stefano, P., 2024. Automatic analysis of pottery sherds based on structure from motion scanning: the case of the phoenician carinated-shoulder amphorae from Tell el-Burak (Lebanon). *J. Cult. Herit.* 67, 336–351. <https://doi.org/10.1016/j.culher.2024.03.012>.
- Fusek, G., 1994. Slovensko Vo Včasnoslovenskom Období. Nitra.
- Gajski, D., Solter, A., Gasparovic, M., 2016. Applications of macro photogrammetry in archaeology. *ISPRS - Int. Arch. Photogramm. Remote Sens. Spatial Informat. Sci.* 41-B5, 263–266.
- Geng, L., Lee, R., Zhang, X., 2024. RayJoin: fast and precise spatial join. In: Proceedings of the 38th ACM International Conference on Supercomputing (ICS '24). Association for Computing Machinery, New York, NY, pp. 124–136. <https://doi.org/10.1145/3650200.3656610>.
- Gojda, M., 1991. Early medieval settlements in Roztoky (the 1986–89 excavation). In: *Archaeology in Bohemia 1986–1990*, pp. 135–139.
- Gower, J.C., 1971. A General Coefficient of Similarity and Some of Its Properties. *Biometrics* 27 (4), 857–871. <https://doi.org/10.2307/2528823>.
- Gravel-Miguel, C., Cristiani, E., Hodgkins, J., Orr, C., Strait, D., Peresani, M., Benazzi, S., Pothier-Bouchard, G., Keller, H., Meyer, D., Drohobytsky, D., Talamo, S., Panetta, D., Zupancich, A., Miller, C., Negrino, F., Riel-Salvatore, J., 2022. The ornaments of the Arma Veiranca early Mesolithic infant burial. *J. Archaeol. Method Theor.* 30. <https://doi.org/10.1007/s10816-022-09573-7>.
- Gualandi, M.L., Gattiglia, G., Anichini, F., 2021. An open system for collection and automatic recognition of pottery through neural network algorithms. *Heritage* 4 (1), 140–159. <https://doi.org/10.3390/heritage4010008>.
- Harush, O., Glauber, N., Zoran, A., Grossman, L., 2019. On quantifying and visualizing the potter's personal style. *J. Archaeol. Sci.* 108, 1–8. <https://doi.org/10.1016/j.jas.2019.104973>.
- HIGGSAS, 2024. Internet manual for Higgsas toolkit. Available at: [https://higgsas-ge-o-nodes-manual.readthedocs.io/en/latest/geometry\\_measure.html#line-plane-intersection](https://higgsas-ge-o-nodes-manual.readthedocs.io/en/latest/geometry_measure.html#line-plane-intersection).
- Hodson, F.R., Sneath, F.H.A., Doran, J.E., 1971. Pokusy o numerickou analýzu archeologických dat. In: Bouzek, J., Buchvaldek, M. (Eds.), *Nové Archeologické Metody I. Trídení Materiálu*, pp. 101–121. Praha.
- Horn, C., Pitman, D., Potter, R., 2019. An evaluation of the visualisation and interpretive potential of applying GIS data processing techniques to 3D rock art data. *J. Archaeol. Sci. Report* 27, 101971. <https://doi.org/10.1016/j.jasrep.2019.101971>.
- Howard, H., 1981. In the wake of distribution: towards an integrated approach to ceramic studies in prehistoric Britain. In: Howard, H., Morris, E.L. (Eds.), *Production and Distribution: a Ceramic Viewpoint*, vol. 120, pp. 1–30. BAR S.
- Jelíneková, D., 2012. K otázce datování počátků kultury s keramikou pražského typu na Moravě. *Přehled výzkumu* 53, 7–21.
- Jiang, X., Peng, Q., Cheng, X., Dai, N., Cheng, C., Li, D., 2016. Efficient booleans algorithms for triangulated meshes of geometric modeling. *Comp.-Aided Des. Appl.* 13 (4), 419–430. <https://doi.org/10.1080/16864360.2015.1131530>.
- Karasik, A., Smilansky, U., 2008. 3D scanning technology as a standard archaeological tool for pottery analysis: practice and theory. *J. Archaeol. Sci.* 35, 1148–1168. <https://doi.org/10.1016/j.jas.2007.08.008>.
- Koštál, M., Nosek, V., Macháček, J., 2025. "Supplementary data for advancing the morphometric analysis of early medieval Slavic pottery: a semi-automated 3D toolset for virtual sections. *J. Archaeol. Sci.* <https://doi.org/10.5281/zenodo.1541117> [Data set].
- Kucukkaya, G., 2004. Photogrammetry and remote sensing in archeology. *J. Quant. Spectrosc. Radiat. Transf.* 88, 83–88. <https://doi.org/10.1016/j.jqsrt.2003.12.030>.
- Kuna, M., Profantová, N., 2005. Počátky raného středověku v Čechách. *Archeologický Výzkum Sídlení Aglomerace Kultury Pražského Typu V Roztokách*. Praha.
- Kuna, M., Hajnalová, M., Kováčiková, L., Lisá, L., Novák, J., Bureš, M., Cílek, V., Hošek, J., Kočář, P., Majer, A., Makowiecki, D., Cummings, L.S., Šuvová, Z., Světlík, I., Vandenberghe, D., Van Nieuland, J., Yost, C.L., Zabílska-Kunek, M., 2013. The early medieval site at roztoky. The evidence of ecofacts. *Památky Archeologické* 104, 59–147.
- Legendre, P., Legendre, L., 1998. *Numerical Ecology*, 2nd English ed. Elsevier, Amsterdam.
- Loftus, J.F., 2022. Reexamining ceramic standardization during agricultural transition: a geometric morphometric investigation of initial – early yayoi earthenware, Japan. *Open Archaeol.* 8 (1), 1249–1268. <https://doi.org/10.1515/opar-2022-0273>.
- Macháček, J., 1997. Metoda základního zpracování archeologických vědeckých dat s pomocí počítačové podpory. In: *Počítačová Podpora V Archeologii*, pp. 33–45. Brno.
- Macháček, J., Eichert, S., Nosek, V., Pernicka, E., 2024. Copper-alloy bell fittings and elite networking in early medieval central Europe. *J. Archaeol. Sci.* 161 (1), 1–12. <https://doi.org/10.1016/j.jas.2023.105895>.
- Mara, H., Bogacz, B., 2022. Digital assyriology—advances in visual cuneiform analysis. *J. Comput. Cult. Herit.* 15, 1–22. <https://doi.org/10.1145/3491239>.
- McCarthy, J., 2014. Multi-image photogrammetry as a practical tool for cultural heritage survey and community engagement. *J. Archaeol. Sci.* 43, 175–185. <https://doi.org/10.1016/j.jas.2014.01.010>.
- Möller, T., Trumbore, B., 1997. Fast, minimum storage ray-triangle intersection. *J. Graph. Tool.* 2 (1), 21–28. <https://doi.org/10.1080/10867651.1997.10487468>.
- Nicholas, J., 2004. *The Second Derivative and Points of Inflection*. University of Sydney, Sydney.
- Nievergelt, J., Preparata, F.P., 1982. Plane-sweep algorithms for intersecting geometric figures. *Commun. ACM* 25 (10), 739–747. <https://doi.org/10.1145/358656.358681>.

- Nosek, V., Kanáková Hladíková, L., 2021. Analytical potential of 3D data in the ballistic analyses of lithic projectiles. *J. Archaeol. Sci.: Report* 38, 1–7. <https://doi.org/10.1016/j.jasrep.2021.103042>.
- Novaković, P., Hornak, M., Zachar, M. (Eds.), 2017. 3D Digital Recording of Archaeological, Architectural and Artistic Heritage. Ljubljana. <https://doi.org/10.4312/9789612378981>.
- Orton, C., Tyers, P., Vince, A., 1993. Pottery in Archaeology. Cambridge Manuals in Archaeology. Cambridge University Press, London.
- Parczewski, M., 1993. Die Anfänge der frühslawischen Kultur in Polen. In: Veröffentlichungen der österreichischen Gesellschaft für Ur- und Frühgeschichte, Band XVII. Österreichischen Gesellschaft für Ur- und Frühgeschichte, Wien.
- Parczewski, M., 2004. Slavs and the early slav culture. In: Bogucki, P.I., Crabtree, P.J. (Eds.), *Ancient Europe 8000 B.C.–A.D. 1000: Encyclopedia of the Barbarian World*. Thompson/Gale, New York, pp. 414–417.
- Petrinelli Pannocchia, C., Vassanelli, A., Terranova, A., et al., 2024. 3D imaging application to the study of the early Neolithic ceramic complex: the decorated pottery of Rio Tana (Abruzzi, Italy). *Europ. Phys. J. Plus* 139, 474. <https://doi.org/10.1140/epjp/s13360-024-05198-9>.
- Pleterski, A., 2009. The inventing of slavs or inventive slavs? O ideovém světě a způsobu bydlení starých Slovanů. *Archeol. Rozhl.* 61 (2), 331–336.
- Poigt, T., Comte, F., Adam, L., 2021. How accurate was Bronze Age weighing in Western Europe? *J. Archaeol. Sci.: Report* 40, 103221. <https://doi.org/10.1016/j.jasrep.2021.103221>.
- Poulík, J., 1951. Staroslovanské mohylové pohřebiště v přítlukách na moravě. *Archeol. Rozhl.* 3, 97–100.
- Rice, P.M., 1981. Evolution of specialized pottery production: a trial model. *Curr. Anthropol.* 22, 219–240.
- Rice, P.M., 1987. Pottery Analysis: a Sourcebook. The University of Chicago Press, Chicago.
- Rusanova, I.P., 1973. Slavianskie Drevnosti VI–IX Vv. Mezhdunarodnij Dneprom i Zapadnym Bugom. Nauka, Moscow.
- Rusanova, I.P., 1976. Slavianskie Drevnosti VI–VII Vv. Kul'Tura Prazhskogo Tipa. Nauka, Moscow.
- Segura, R., Feito, F., 2001. Algorithms to test ray-triangle intersection: comparative study. *J. WSCG* 9 (3), 76–81.
- Shepard, A.O., 1971. Ceramics for the Archaeologist. Carnegie Institution, Washington D. C.
- Smith, M.P., 1985. Toward an economic interpretation of ceramics: relating vessel size and shape to use. In: Nelson, B.A. (Ed.), *Decoding Prehistoric Ceramics*, vol. 1985. Southern Illinois University Press, Center for Archaeological Investigations, Carbondale, pp. 254–437.
- Slavíček, K., Těsnohlídková, K., Košťál, M., Václavíková, D., Trnová, K., 2024. A pottery kiln from the second half of the 13th century in Zdár nad Sázavou – Staré město (Czech republic): technological analysis of its batch. *Archeol. Rozhl.* 75 (4), 403–438.
- Šindelář, J., Poláček, L., Krupičková, Š., 2019. Doporučená metodika Fotodokumentace v archeologii pro Následné Metrické Analýzy obrazu. *Přehled výzkumu* 60 (2), 201–224.
- Thér, R., Wilczek, J., 2022. Identifying the contribution of rotational movement in pottery forming based on statistical surface analysis. *Archaeol. Anthropol. Sci.* 14. <https://doi.org/10.1007/s12520-022-01561-y>.
- Tsiafaki, D., Michailidou, N., 2015. Benefits and problems through the application of 3D technologies in archaeology: recording, visualisation, representation and reconstruction. *Scientific Culture* 1 (3), 37–45. <https://doi.org/10.5281/zenodo.18448>.
- Wang, L., Marwick, B., 2020. Standardization of ceramic shape: a case study of Iron Age pottery from northeastern Taiwan. *J. Archaeol. Sci.: Report* 33, 102554. <https://doi.org/10.1016/j.jasrep.2020.102554>.
- Wilczek, J., Monna, F., Barral, P., Burlet, L., Chateau, C., Navarro, N., 2014. Morphometrics of second Iron Age ceramics – strengths, weaknesses, and comparison with traditional typology. *J. Archaeol. Sci.* 50, 39–50. <https://doi.org/10.1016/j.jas.2014.05.033>.
- Zapassky, E., Finkelstein, I., Benenson, I., 2006. Ancient standards of volume: Negevite Iron Age pottery (Israel) as a case study in 3D modeling. *J. Archaeol. Sci.* 33 (12), 1734–1743. <https://doi.org/10.1016/j.jas.2006.03.005>.
- Zoll-Adamikowa, H., 1977. Próba klasyfikacji typologicznej ceramiki słowiańskiej w VI–VII w. Na przykładzie materiałów z dorzecza górnej Wisły. Referat zo Sympozia „Slovenská Keramika 5.–8. Stor in Moscow 1977; manuscript.